

# Safe Sequential Trajectory Planning of Multi-Vehicle Systems via Hamilton-Jacobi-Isaacs Variational Inequality

Mo Chen, Jaime Fernandez Fisac, Shankar Sastry, Claire J. Tomlin

**Abstract**—We consider the problem of planning trajectories for a group of  $N$  vehicles, each aiming to reach its target set while avoiding danger zones of all other vehicles. The analysis of problems like this is extremely important practically, especially with the growing interest in utilizing unmanned aircraft systems for civil purposes. The direct solution of this problem by solving an Hamilton-Jacobi-Isaacs (HJI) partial differential equation (PDE) is numerically intractable due to the exponential scaling of computation complexity with problem dimensionality. Furthermore, the traditional terminal value HJI PDE cannot directly handle the case where vehicles do not have a common scheduled arrival time. Instead, we perform sequential trajectory planning by considering vehicles in order of priority, modeling higher-priority vehicles as time-varying obstacles. To do this, we solve a double-obstacle HJI variational inequality (VI) which computes the reach-avoid set, defined as the set of states from which a vehicle can reach its target while staying within a time-varying state constraint set. From the solution of the HJI VI, we can also extract the latest acceptable departure time and the optimal control for each vehicle. This is a first application of the double-obstacle HJI VI which can handle systems with time-varying dynamics, target sets, and state constraint sets, and results in computation complexity that scales linearly, as opposed to exponentially, with the number of vehicles in consideration.

## I. INTRODUCTION

Consider a group of autonomous vehicles trying to perform a task or reach a goal, which may be static or time-varying in the joint state space of the vehicles. In addition, the vehicles must avoid obstacles, and other vehicles. Providing safety and performance guarantees for such a multi-agent autonomous system is very relevant practically. UAVs, for example, have in the past been used mainly for military operations [1]. However, recently, there has been a growing interest in using UAVs for civil applications, as companies like Amazon and Google are looking in the near future to send unmanned aerial vehicles into the airspace to deliver packages [2], [3]. Because of this, government agencies such as the FAA are also very interested in analyzing these problems in order to prevent conflicts in the airspace with the introduction of potentially many UAVs in an urban environment [4]. In addition, UAVs can be used not only to deliver packages quickly, but in any situation where fast response is desired. For example, UAVs can provide

emergency supplies to disaster-struck areas that are otherwise difficult to reach [5].

In general, multi-agent systems are difficult to analyze due to their inherent high dimensionality. For example, the joint state space of 10 vehicles would have 30 dimensions if each vehicle can be described by 3 dimensions. Multi-vehicle systems also often involve aspects of cooperation and asymmetric goals among the vehicles or teams of vehicles, making their analysis particularly interesting. Despite these difficulties, it is still important to analyze multi-agent autonomous systems because of their applications in robotics and aircraft safety.

Multi-agent autonomous systems have been explored extensively in the literature. Some researchers have done work on multi-vehicle path planning in the presence of other vehicles with assumptions on specific control strategies of unknown vehicles or moving obstacles [6], [7]. Others have used potential functions to guarantee collision avoidance while maintaining formation given a predefined trajectory [8], [9]. However, these bodies of work have not considered trajectory planning and collision avoidance simultaneously.

One well-known technique for optimal trajectory planning under disturbances or adversaries is reachability analysis, in which one computes the reach-avoid set, defined as the set of states from which the system can reach a target set while remaining within a state constraint set for all time. For reachability of systems of up to five dimensions, the Hamilton-Jacobi formulation of dynamic games [10], [11] have been used in situations where obstacles and target sets are static. HJI variational inequalities (VI) have also been used in this case [12], [13]. The HJI VI formulation in [12] is able to handle moving target sets with no obstacles, while the formulation in [13] is able to handle static target sets and static obstacles.

The above-mentioned approaches for computing reach-avoid sets are practically appealing due to the availability of modern numerical tools such as [14], [15], [10], [16], which are able to solve the HJI equations when the dimensionality of the problem is low. These numerical tools have been successfully used to solve a variety of differential games, path planning problems, and optimal control problems, including aircraft collision avoidance [10], automated in-flight refueling [17], and two-player reach-avoid games [18]. The advantage of the HJI approaches is that they can be applied to a large variety of system dynamics, and provides guarantees on the system's safety and performance.

Despite the power of the HJI approaches for the analysis of low dimensional systems, the approaches become numer-

This work has been supported in part by NSF under CPS:ActionWebs (CNS-931843), by ONR under the HUNT (N0014-08-0696) and SMARTS (N00014-09-1-1051) MURIs and by grant N00014-12-1-0609, by AFOSR under the CHASE MURI (FA9550-10-1-0567). The research of J.F. Fisac has received funding from the "la Caixa" Foundation.

All authors are with the Department of Electrical Engineering and Computer Sciences, University of California, Berkeley. {jfisac, mochen72, tomlin, sastry}@eecs.berkeley.edu

ically intractable very quickly as the number of vehicles in the system is increased. This is because the numerical computations are done on a grid in the joint state space of the system, resulting in an exponential scaling of computation complexity with respect to the dimensionality of the problem. Furthermore, state constraint sets, while useful for modeling unsafe vehicle configurations, are required to be time-invariant in [10], [11], [13]. To solve problems involving time-varying state constraints, [19] proposed to augment state space with time; however, this introduces an extra state space dimension without addressing the added computation complexity.

Recently, [?] presented a double-obstacle HJI VI which handles problems in which the dynamics, target sets, and state constraint sets are all time-varying, and provided a numerical implementation based on well-known schemes. The formulation does not introduce any additional computation overhead compared to the above-mentioned techniques, while maintaining the same guarantees on the system's safety and performance. Now, we provide a first application of the theory presented in [?].

Our contributions in this paper are as follows. First, we formulate a multi-vehicle collision avoidance problem involving  $N$  autonomous vehicles. Each vehicle seeks to get to its own target sets while avoiding collision with all other vehicles. To reduce the problem complexity to make the problem tractable, we assign a priority to each vehicle, and model other vehicles as time-varying obstacles that need to be avoided. We then utilize the double-obstacle HJI VI proposed in [?] to compute reach-avoid sets to plan trajectories for vehicles in order of priority. This way, we are able to offer a tractable solution that scales linearly, as opposed to exponentially, with the number of vehicles. We compare our approach to the traditional HJI approach involving static obstacles in a simple two-vehicle system, and demonstrate the scalability of our approach in a more complex four-vehicle system.

## II. PROBLEM FORMULATION

Consider  $N$  vehicles  $P_i, i = 1 \dots, N$ , each trying to travel to one of  $N$  destinations, which we will refer to as target sets  $\mathcal{T}_i, i = 1 \dots, N$ , while avoiding collision with each other. Each vehicle  $i$  has states  $\mathbf{x}_i \in \mathbb{R}^{n_i}$  and travels on a domain  $\Omega = \Omega_{obs} \cup \Omega_{free}$ , where  $\Omega_{obs}$  represent the obstacles that each vehicle must avoid, and  $\Omega_{free}$  represents all other states in the domain at which vehicles can move. Each vehicle  $i = 1, 2, \dots, N$  moves with the following dynamics for  $t \in [t_i^i, t_i^f]$ :

$$\begin{aligned} \dot{\mathbf{x}}_i &= f_i(\mathbf{x}_i, \mathbf{u}_i), \\ \mathbf{x}_i(t_i^i) &= \mathbf{x}_i^0 \end{aligned} \quad (1)$$

where  $\mathbf{x}_i^0$  represents the initial condition of vehicle  $i$ ,  $\mathbf{u}_i(\cdot)$  represents the control functions of vehicle  $i$ . In general,  $f_i(\cdot, \cdot)$  depends on the specific dynamic model of vehicle  $i$ , and need not be of the same form across different vehicles. Denote  $\mathbf{p}_i$  the subset of the states  $\mathbf{x}_i$  to be the position of the

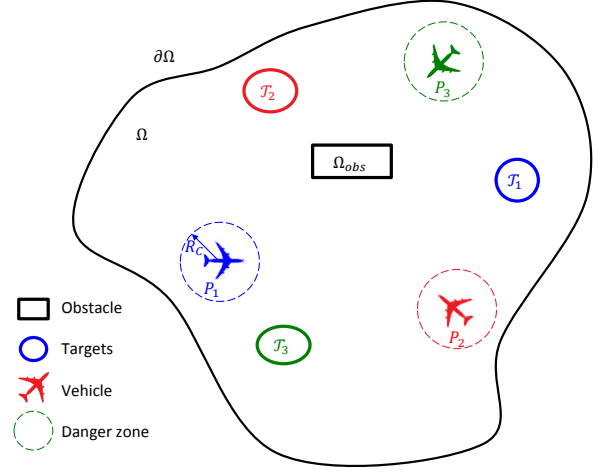


Fig. 1: An illustration of the problem formulation with 3 vehicles. Each vehicle  $P_i$  seeks to reach its target set  $\mathcal{T}_i$  by time  $t = t_i^f$ , while avoiding physical obstacles  $\Omega_{obs}$  and the danger zones of other vehicles.

vehicle. Given  $\mathbf{p}_i^0 \in \Omega_{free}$ , we define the admissible control function set for  $P_i$  to be the set of all control functions such that  $\mathbf{p}_i(t) \in \Omega_{free} \forall t \geq 0$ . Denote the joint state space of all vehicles  $\mathbf{x} \in \mathbb{R}^n$  where  $n = \sum_i n_i$ , and their joint control  $\mathbf{u}$ .

We assume that the control functions  $\mathbf{u}_i(\cdot)$  are drawn from the set  $\mathbb{U}_i := \{\mathbf{u}_i : [t_i^i, t_i^f] \rightarrow \mathcal{U}_i, \text{measurable}\}$  where  $\mathcal{U}_i \in \mathbb{R}^{n_i^u}$  is the set of allowed control inputs. Furthermore, we assume  $f_i(\mathbf{x}_i, \mathbf{u}_i)$  Lipschitz continuous in  $\mathbf{x}_i$  for any fixed  $\mathbf{u}_i$ , and therefore given any initial state  $\mathbf{x}_i^0$  and any control function  $\mathbf{u}_i(\cdot)$ , there exists a unique, continuous trajectory  $\mathbf{x}_i(\cdot)$  solving (1) [20].

The goal of each vehicle  $i$  is to arrive at  $\mathcal{T}_i \subset \mathbb{R}^{n_i}$  at some pre-specified time  $t_i^f$  in minimum time (i.e. while minimizing  $t_i^f - t_i^i$ ), while avoiding danger with all other vehicles. The target sets  $\mathcal{T}_i$  can be used to represent desired kinematics quantities such as position and velocity, and, in the case of non-holonomic systems, quantities such as heading angle.  $t_i^f$  can be interpreted as the scheduled arrival time of vehicle  $i$ , and  $t_i^i$  can be interpreted as the latest acceptable departure time for vehicle  $i$ . Thus, our problem can be thought of as determining the latest acceptable departure time  $t_i^i$  for each vehicle such that each vehicle can get to  $\mathcal{T}_i$  at or before  $t_i^f$ , and finding a control to do this safely.

Danger is described by sets  $\mathcal{D}_{ij}(\mathbf{x}_j) \subset \Omega$ . In general, the definition of  $\mathcal{D}_{ij}$  depends on the conditions under which one considers vehicles  $i$  and  $j$  to be in an unsafe configuration, given the state of vehicle  $j$ . In this paper, we consider vehicles  $i$  and  $j$  to be in an unsafe configuration if the positions of the two vehicles come within a certain radius  $R_C$ :  $\mathcal{D}_{ij}(\mathbf{x}_j) = \{\mathbf{x}_i : \|\mathbf{p}_i - \mathbf{p}_j\|_2 \leq R_C\}$ .

An illustration of the problem setup is shown in Figure 1.

In general, the analysis of the above problem in general must be done in the joint state-space of all vehicles, making the analysis computationally intractable. In this paper, we

will instead consider the problem of performing path planning of the vehicles in a sequential manner. Without loss of generality, we consider the problem of first fixing  $i = 1$  and determining the optimal control for vehicle 1, the vehicle with the highest priority. The resulting optimal control  $\mathbf{u}_1$  sends vehicle 1 to  $\mathcal{T}_1$  in minimum time.

Then, we plan the minimum time trajectory for each vehicle  $i = 2, 3, \dots, N$ , in that order, given the trajectories for higher-priority vehicles  $1, 2, \dots, i-1$ . We assume that all vehicles have complete information about the states and trajectories of all other vehicles, and that all vehicles adhere to their planned trajectories. Thus, in planning its trajectory, vehicle  $i$  treats higher-priority vehicles  $1, 2, \dots, i-1$  as time-varying obstacles.

With the above sequential path planning protocol and assumptions, our problem now reduces to the following for vehicle  $i$ . Given  $\mathbf{x}_j(\cdot), j = 1, \dots, i-1$ , determine  $\mathbf{u}_i(\cdot)$  that maximizes  $t_i^f$  and such that  $\mathbf{x}_i(t_i^f) \in \mathcal{T}_i$ .

### III. SOLUTION VIA VARIATIONAL INEQUALITY AND SEQUENTIAL PATH PLANNING

One direct way of solving the problem formulated in Section II is by solving a corresponding HJI PDE [10]. In this approach, one considers the joint dynamics of the entire system,  $f(\mathbf{x}, \mathbf{u})$ , and define the goal set and the avoid set in the joint state space of all vehicles. The goal set encodes the joint states representing all vehicles being at their target sets, and the avoid set encodes the joint states representing all unsafe configurations. These sets are defined as sub-zero-level sets of appropriate implicit surface functions  $s(\mathbf{x})$  where  $\mathbf{x} \in \mathcal{S} \Leftrightarrow s(\mathbf{x}) \leq 0$ . Having defined the implicit surface functions, the HJI PDE (2) is then solved backwards in time with the terminal set as the initial condition and the avoid set as a constraint to obtain the reach-avoid set  $\mathcal{RA}$ , which defines the set of states from which the system has a control to drive the state to the goal set  $\mathcal{L}$  while staying out of the avoid set  $\mathcal{A}$  all times.

$$\frac{\partial V}{\partial t} + \min \left[ 0, H \left( \mathbf{x}, \frac{\partial V}{\partial \mathbf{x}} \right) \right] = 0, \quad V(\mathbf{x}, 0) = l(\mathbf{x}) \quad (2)$$

subject to  $\Phi(\mathbf{x}, t) \geq -a(\mathbf{x})$

where the optimal Hamiltonian is given by

$$H(\mathbf{x}, p) = \min_{\mathbf{u} \in \mathcal{U}} p \cdot f(\mathbf{x}, \mathbf{u}).$$

The direct solution described above has been successfully used to solve a number of problems involving up to a pair of vehicles [10], [17], [18], [21]. However, since the numerical methods for solving the HJI PDE involves gridding up the state space, the computation complexity scales exponentially with the number of dimensions in the joint state. This makes the HJI PDE inapplicable for problems involving three or more vehicles. Therefore, instead of solving an HJI PDE in the joint state space in  $\mathbb{R}^n = \mathbb{R}^{\sum_i n_i}$ , we will consider the problem in  $\mathbb{R}^{n_i}$  and solve a sequence of double-obstacle HJI VIs introduced in [?]. By doing so, we take advantage of the fact that time-varying targets, obstacles,

and dynamics can be handled by the double-obstacle HJI VIs (but not by the HJI PDE), making the analysis of the problem tractable. Furthermore, even if the dimensionality of the problem is sufficiently low for computing a numerical solution to the HJI PDE, the inability to handle time-varying systems would still limit the HJI PDE to be useful only for solving problems in which the required time of arrival is common to all vehicles:  $t_i^f = t^f \forall i$ .

We first describe the framework for computing reachable sets with arbitrary terrain, domain, moving obstacles, and moving target sets based on [?]. As with the HJI PDE, sets are also defined as sub-zero-level sets of implicit surface functions; however, crucially, unlike in the HJI PDE, these implicit surface functions can be time-varying in the HJI VI. Being able to compute reach-avoid sets with moving obstacles allows us to overcome the computational intractability described above by sequentially performing path planning for one vehicle at a time in order of priority, while treating higher-priority vehicles as moving obstacles. The target set is defined in the same way as in the HJI PDE; the avoid set is by convention defined as the complement of the state constraint set in the HJI VI.

#### A. Reachability via HJI VI

We first state the result given in [?], and then specialize the result to the problem formulation given in Section II. Consider a general nonlinear system describing the state evolution of two players in a differential game in the time horizon  $t \in [0, T]$ .

$$\dot{x}(t) = f(t, x, u, d), x(0) = x \quad (3)$$

where  $x$  is the joint state,  $u$  is the control input for player 1, and  $d$  is the control input for player 2. Their joint dynamics  $f$  is assumed to be Lipschitz continuous in  $x$  for any fixed  $u, d$  and  $t$ . Given control functions  $u(\cdot), d(\cdot)$ , there exists a unique trajectory  $\phi_x^{u,d}(\tau, \tau)$  [20]. Player 1 wishes to minimize, and player 2 wishes to maximize the following cost functional:

$$\begin{aligned} \mathcal{V}(t, x, u(\cdot), d(\cdot)) \\ = \min_{\tau \in [t, T]} \max \left\{ l(\phi_{x(0)}^{u,d}(\tau, \tau)), \max_{s \in [t, \tau]} g(\phi_{x(0)}^{u,d}(s), s) \right\} \end{aligned} \quad (4)$$

The outcome, or value of the game, is given by

$$V(x, t) := \sup_{u(\cdot)} \inf_{d(\cdot)} \mathcal{V}(x, t, u(\cdot), d(\cdot)) \quad (5)$$

The value of the game characterizes reach-avoid set, or all the states from which player 1 can reach the target  $\mathcal{L}$  encoded by the implicit surface function  $l(x, t)$ , while staying within some state constraint set  $\mathcal{G}$  encoded by the implicit surface function  $g(x, t)$ , despite the adversarial actions of player 2. The value function is the unique viscosity solution [22] to the following HJI VI [?]:

$$\begin{aligned} \max \left\{ \min \left\{ \partial_t V + H^\pm(x, D_x V, t), l(x, t) - V(x, t) \right\} \right. \\ \left. g(x, t) - V(x, t) \right\} = 0, \quad t \in [0, T], x \in \mathbb{R}^n \\ V(x, T) = \max \{l(x, T), g(x, T)\}, \quad x \in \mathbb{R}^n \end{aligned} \quad (6)$$

The proof is given in [?] and is based on [12], [13].

Now consider the nonlinear system with dynamics given by (1). Given a time-varying target set  $\mathcal{T}_i(t)$ , we define an implicit surface function  $l(\mathbf{x}_i, t)$  such that  $\mathbf{x}_i \in \mathcal{T}_i(t) \Leftrightarrow l_i(\mathbf{x}_i, t) \leq 0$ . Given a time-varying obstacle  $\mathcal{A}_i(t)$  that the vehicle  $i$  must avoid, we define another implicit surface function  $g_i(\mathbf{x}_i, t)$  such that  $\mathbf{x} \notin g_i(\mathbf{x}, t) \Leftrightarrow g_i(x, t) \leq 0$ . With the above definitions, the problem formulated in Section II is equivalent to the optimal control problem in which vehicle  $i$  chooses a control function  $\mathbf{u}_i(\cdot)$  to minimize the following cost functional:

$$\begin{aligned} \mathcal{V}_i(t, \mathbf{x}_i, \mathbf{u}_i(\cdot)) \\ = \min_{\tau \in [t, T]} \max \left\{ l_i(\mathbf{x}_i(\tau), \tau), \max_{s \in [t, \tau]} g_i(\mathbf{x}_i(s), s) \right\} \end{aligned} \quad (7)$$

Note here, we have an optimal control problem involving only one vehicle and no adversary, unlike in the case of the HJI VI (6). Now, specializing (6) to our optimal control problem, the value function that characterizes the reach-avoid set  $\mathcal{RA}_i(t)$  is given by  $V_i(\mathbf{x}_i, t)$ , where  $\mathbf{x}_i \in \mathcal{RA}_i(t) \Leftrightarrow V_i(\mathbf{x}_i, t) \leq 0$ .  $V_i(\mathbf{x}_i, t)$  is the viscosity solution [22] of the HJI VI

$$\begin{aligned} \max \left\{ \min \left\{ \partial_t V_i + H_i(\mathbf{x}_i, D_{\mathbf{x}_i} V_i, t), l_i(\mathbf{x}_i, t) - V_i(\mathbf{x}_i, t) \right\} \right. \\ \left. g_i(\mathbf{x}_i, t) - V_i(\mathbf{x}_i, t) \right\} = 0, t \in [t_i^i, t_i^f], \mathbf{x}_i \in \mathbb{R}^{n_i} \\ V_i(\mathbf{x}_i, t_i^f) = \max \left\{ l_i(\mathbf{x}_i, t_i^f), g_i(\mathbf{x}_i, t_i^f) \right\}, \quad \mathbf{x}_i \in \mathbb{R}^{n_i} \end{aligned} \quad (8)$$

where the Hamiltonian  $H_i(t, \mathbf{x}_i, p)$  is given by

$$H_i(t, \mathbf{x}_i, p) = \min_{\mathbf{u}_i \in \mathcal{U}_i} p \cdot f_i(t, \mathbf{x}_i, \mathbf{u}_i)$$

### B. Sequential Path Planning

To use (8) to perform sequential path planning of vehicles, we first define the moving obstacles induced by higher-priority vehicles. Specifically, for vehicle  $i$ , we define the moving obstacles  $\mathcal{O}_j^i(t)$  induced by vehicles  $j = 1, \dots, i-1$  given their known trajectories  $\mathbf{x}_j(\cdot)$  to be

$$\mathcal{O}_j^i(t) := \{\mathbf{x}_i : \mathbf{p}_i \in \mathcal{D}_{ij}(\mathbf{x}_j(t))\} \quad (9)$$

Each vehicle  $i$  must avoid being in  $\mathcal{O}_j^i(t)$  for each  $j = 1, \dots, i-1$  and for all time  $t$ , as well as avoid being in static obstacles  $\Omega_{obs}$  in the domain.

Therefore, for the  $i^{\text{th}}$  vehicle, we compute the reach-avoid set with the time-varying avoid set

$$\mathcal{A}_i(t) := \{\mathbf{x}_i : \mathbf{p}_i \in \Omega_{obs}\} \cup \left( \bigcup_{j=1, \dots, i-1} \mathcal{O}_j^i(t) \right) \quad (10)$$

and the time-varying goal set

$$\mathcal{L}_i(t) := \mathcal{T}_i \setminus \mathcal{A}_i(t) \quad (11)$$

The goal set is represented by the implicit surface function  $l_i(\mathbf{x}_i, t)$ , where  $l_i(\mathbf{x}_i, t) \leq 0 \Leftrightarrow \mathbf{x}_i(t) \in \mathcal{L}_i(t)$ . The state constraint set in the HJI VI is defined as the complement of the avoid set,  $\mathcal{A}_i^c(t)$ , and is represented by the implicit surface function  $g(\mathbf{x}_i, t)$ , where  $g(\mathbf{x}_i, t) \leq 0 \Leftrightarrow \mathbf{x}_i \notin \mathcal{A}_i(t)$ . For both  $l_i(\mathbf{x}_i, t)$  and  $g(\mathbf{x}_i, t)$ , we use the signed distance function (in  $\mathbf{x}_i$ ) to the sets  $\mathcal{L}_i(t)$  and  $\mathcal{A}_i^c(t)$ , respectively.

Now, we can solve the HJI VI (8). The solution  $V(\mathbf{x}_i, t)$  represents the reach-avoid set  $\mathcal{RA}(t)$ :  $V(\mathbf{x}_i, t) \leq 0 \Leftrightarrow \mathbf{x}_i(t) \in \mathcal{RA}(t)$ .  $\mathcal{RA}(t)$  is the set of states at starting time  $t$  from which vehicle  $i$  can arrive at  $\mathcal{T}_i$  at time  $t_i^f$  while avoiding obstacles and danger zones of all higher-priority vehicles  $j = 1, \dots, i-1$ .

Alternatively, given an initial state  $\mathbf{x}_i^0$ , we can solve (8) to some  $t_i^i = \inf\{t : \mathbf{x}_i^0 \in \mathcal{RA}(t)\}$ . This represents the latest time that vehicle  $i$  must depart from its initial position in order to reach  $\mathcal{T}_i$  while avoiding all danger zones of higher-priority vehicles  $j = 1, \dots, i-1$ .

The optimal control that minimizes the time to reach  $\mathcal{T}_i$  is given by

$$\mathbf{u}_i(t) = \arg \min H_i(t, \nabla_{\mathbf{x}_i} V(\mathbf{x}_i, t), V(\mathbf{x}_i, t)) \quad (12)$$

Observe that since each vehicle  $i$  is guaranteed to be safe with respect to higher priority vehicles  $j = 1, \dots, i-1$ , the safety of all vehicles can also be guaranteed.

## IV. NUMERICAL IMPLEMENTATION

For the numerical examples in this paper, we use a numerical scheme provided in [?] which is based on methods in [14], [10]:

$$\begin{aligned} \check{V}(\mathbf{x}_i, t_n) &\leftarrow \min \left\{ D_t \hat{V} + \hat{H}(\mathbf{x}_i, D_x^+ \hat{V}, D_x^- \hat{V}), l(\mathbf{x}_i, t_n) \right\} \\ \hat{V}(\mathbf{x}_i, t_n) &\leftarrow \max \left\{ \check{V}(\mathbf{x}_i, t_n), g(\mathbf{x}_i, t_n) \right\} \end{aligned} \quad (13)$$

where  $\mathbf{i}$  denote the index of the grid point in a discretized computational domain, and  $\check{V}$  represents the intermediate value function that takes into account the target set  $l$  but not the constraint set  $g$ ;  $\hat{V}$  represents the numerical approximation to  $V$ .  $D_x^+ \hat{V}, D_x^- \hat{V}$  represent the “right” and “left” approximations of spatial derivatives. For the numerical Hamiltonian  $\hat{H}$ , we used the well-known Lax-Friedrich approximation [11], [23].

For the spatial derivatives  $D_x^\pm \hat{V}$ , we used a fifth-order accurate weighted essentially nonoscillatory scheme [23], [24]. For the time derivative  $D_t \hat{V}$ , we used a third-order accurate total variation diminishing Runge-Kutta scheme [24], [25]. For these numerical derivative approximations, the



implementation in [16] is used. For two-, three-, and four-dimensional computations, we used a  $200^2, 71^3, 45^4$  grid, respectively.

Note that although the two examples we present have two and four vehicles, our method of solving HJI VI (8) can be done for any number of vehicles, as long as the state space of each vehicle is not too high-dimensional. Thus, the computational complexity of our method scales linearly with the number of vehicles with overlapping time horizons  $[t_i^i, t_i^f]$ , allowing the possibility of performing trajectory planning for a very large number of vehicles.

## V. TWO VEHICLES WITH KINEMATICS MODEL

Consider two vehicles  $i = 1, 2$  using the simple kinematics model with the following dynamics in  $t \in [t_i^i, t_i^f]$ :

$$\begin{aligned} \dot{\mathbf{x}}_i &= v_i \mathbf{u}_i(t), \mathbf{u}_i(t) \in \mathcal{U}_i \\ \mathbf{x}_i(t_i^i) &= \mathbf{x}_i^0 \end{aligned} \quad (14)$$

where  $v_1 = v_2 = 1$  are the maximum speeds of the vehicles and  $\mathcal{U}_i$  is the unit disk. The interpretation of this model is that each vehicle can move in any direction at some maximum speed. With the above dynamics, the Hamiltonian for each vehicle is

$$H_i(t, \nabla_{\mathbf{x}_i} V_i(\mathbf{x}_i, t), V_i(\mathbf{x}_i, t)) = \min_i v_i \mathbf{u}_i(t) \cdot \nabla V(\mathbf{x}_i, t) \quad (15)$$

giving the optimal control

$$\mathbf{u}_i(t) = -\frac{\nabla_{\mathbf{x}_i} V_i(\mathbf{x}_i, t)}{\|\nabla_{\mathbf{x}_i} V_i(\mathbf{x}_i, t)\|_2} \quad (16)$$

The vehicles have the following required times of arrival from the following initial conditions:

$$\begin{aligned} \mathbf{x}_1^0 &= [-0.5 \ 0]^\top \\ \mathbf{x}_2^0 &= [0.5 \ 0]^\top \\ t_1^f &= t_2^f = 0 \end{aligned} \quad (17)$$

The target sets of the vehicles are squares with side length 0.2 on the opposite side of the domain, and the obstacles are rectangles near the middle of the domain. The system's initial conditions and domain are shown in Figure 2.

For this system, we determine  $t_1^i, t_2^i$ , the latest acceptable times that vehicles 1, 2 must depart from their initial positions  $\mathbf{x}_1^0, \mathbf{x}_2^0$  in order to reach their respective targets  $\mathcal{T}_1, \mathcal{T}_2$  while avoiding danger. We will do this by computing the reach-avoid sets from the target sets using two different methods. First, we perform sequential path planning by solving the HJI VI (8) for the two vehicles as outlined in Section III. Second, note that this system has a joint state space of four dimensions, and thus the traditional Hamilton-Jacobi-Isaacs approach [10] would actually be numerically intractable. Therefore, we will also use compute the reach-avoid set by solving the HJI PDE (2) in four dimensions for comparison.

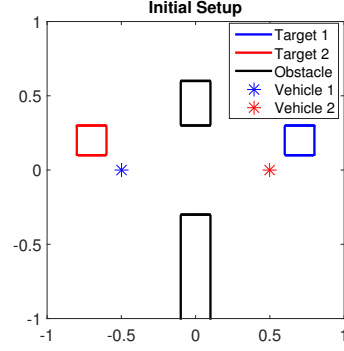


Fig. 2: Initial configuration of the two-vehicle example.

### A. Solution via HJI VI and Sequential Path Planning

With the HJI VI and sequential path planning approach, we first determine the optimal trajectory for vehicle 1 that brings vehicle 1 from  $\mathbf{x}_1^0$  to  $\mathcal{T}_1$  in minimum time. Then, given the trajectory for vehicle 1, we determine the minimum-time trajectory for vehicle 2 that brings vehicle 2 from  $\mathbf{x}_2^0$  to  $\mathcal{T}_2$  while avoiding the danger zone of vehicle 1.

Figure 3 shows the reach-avoid set at various times for vehicle 2. The red square is the target, the black rectangles are the obstacles, and the dashed black circle is the obstacle induced by the trajectory of vehicle 1. We start at  $t = t_2^f = 0$ , and propagate the reach-avoid set backwards in time until  $t = t_2^i = -1.13$ .

Before the induced obstacle touches the reach-avoid set, the reach-avoid set grows from the target set in the same way as in a front propagation problem with uniform speed; this is shown in the left top subplot. Eventually, the obstacle inhibits the propagation of the reach-avoid set, shown in the next two subplots. Finally, the reach-avoid set grows to contain  $\mathbf{x}_2^0$ , and the computation is stopped at  $t_2^i = -1.13$ . The left top plot of Figure 4 shows the resulting trajectory from applying the optimal control in Equation (12).

Computations were done on a  $200^2$  grid with uniform spacing. Trajectory planning for vehicle 1 took approximately 0.34 seconds using the fast marching method [14]. Trajectory planning via solving Equation (8) for vehicle 2 in given the trajectory for vehicle 1 took approximately 25 seconds. Computations were done on a Lenovo T420s laptop with a Core i7-2640M processor. This is orders of magnitude faster than doing a four-dimensional HJI calculation, which takes approximately 30 minutes.

### B. Solution via HJI PDE

To solve the HJI PDE (2), first we define, in the joint state space of the vehicles, the joint target set

$$\mathcal{T} = \{(\mathbf{x}_1, \mathbf{x}_2) \in \mathbb{R}^4 : \mathbf{x}_1 \in \mathcal{T}_1 \wedge \mathbf{x}_2 \in \mathcal{T}_2\} \quad (18)$$

Next we define, also in the joint state space of the vehicles, the *static* joint avoid set

$$\begin{aligned} \mathcal{A} = \{(\mathbf{x}_1, \mathbf{x}_2) \in \mathbb{R}^4 : \mathbf{x}_1 \in \Omega_{obs} \vee \mathbf{x}_2 \in \Omega_{obs} \\ \vee \|\mathbf{x}_1 - \mathbf{x}_2\|_2 \leq R_C\} \end{aligned} \quad (19)$$

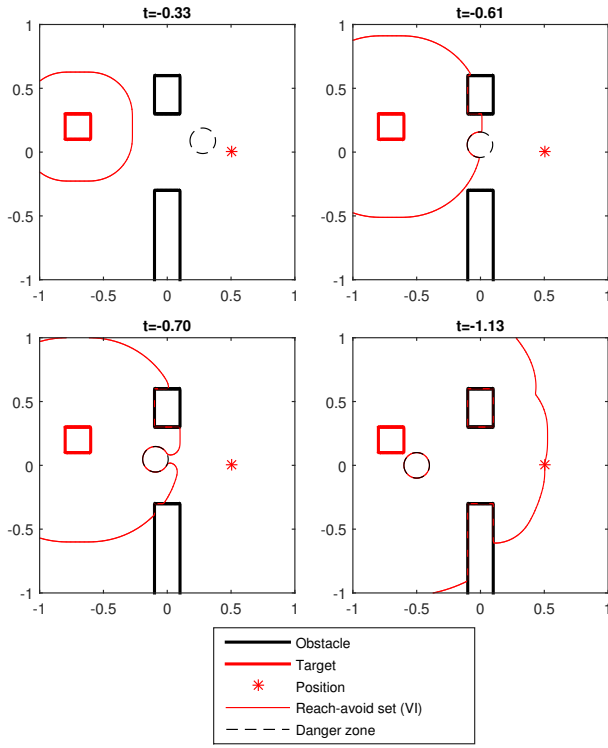


Fig. 3: Evolution of reach-avoid set for vehicle 2. The initial reach-avoid set at time 0 grows backwards in time unobstructed before it encounters obstacles (left top). When the time reaches  $t = -0.61$ , the growth of the reach-avoid set is inhibited by both the static obstacle  $\Omega_{obs}$  and the time-varying obstacle induced by vehicle 1,  $\mathcal{O}_1^1$ . The evolution of the reach-avoid set is computed until  $t = t_2^i = -1.13$ , at which it contains vehicle 2's initial position.

Now, we can solve the HJI PDE (2) with the terminal set  $\mathcal{T} \setminus \mathcal{A}$ , and the avoid set  $\mathcal{A}$ .

The result of solving the HJI PDE is shown in the top right and bottom left subplots of Figure 4. The top right subplot shows the resulting trajectory, in which the two vehicles cooperatively avoid collision. The bottom left plot compares the reach-avoid sets computed from solving the HJI PDE (2) and solving the HJI VI (8) at  $t = t_2^i$ . The two sets are quite similar. The discrepancy between the reach-avoid sets is due to the difference in control strategies derived from the two different approaches: with the HJI PDE, we compute the joint optimal control for both vehicles, and with the HJI VI, we compute the optimal control for vehicle 2 given vehicle 1's optimal trajectory, which does not take into account vehicle 2's motion.

For the latest time of departure, we get  $t_2^i = -1.15$  from the HJI PDE (recall  $t_2^i = -1.13$  from the HJI VI). This discrepancy is likely due to the grid resolution limitation when doing a four-dimensional calculation. Computations were done on a  $45^4$  grid with uniform spacing, and took approximately 30 minutes on a Lenovo T420s laptop with a Core i7-2640M processor.

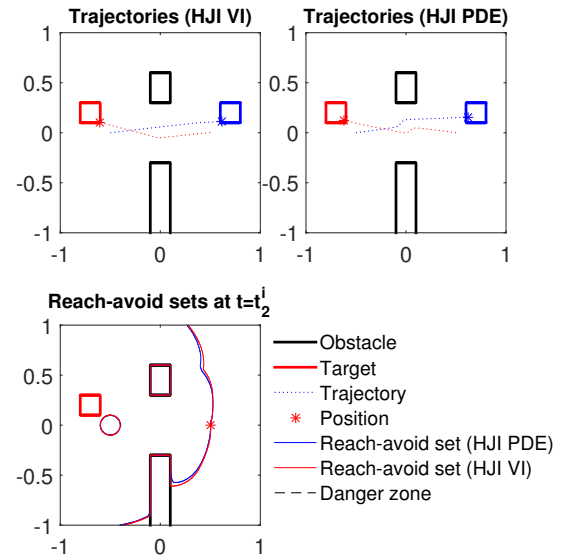


Fig. 4: A comparison between the HJI VI solution and the HJI PDE solution. Using the HJI VI solution, vehicle 1 moves towards  $\mathcal{T}_1$  along the shortest path, disregarding the actions of vehicle 2, which optimally moves to  $\mathcal{T}_2$  while avoiding vehicle 1. Using the HJI PDE solution, both vehicles avoid each other along their trajectory to the targets. The resulting reach-avoid sets at  $t = t_2^i$  are very similar.

## VI. FOUR VEHICLES WITH CONSTRAINED TURN RATE

In this example, we have four vehicles with states  $\mathbf{x}_i = [x_i, y_i, \theta_i]^T$  modeled using a horizontal kinematics model with the following dynamics for  $t \in [t_i^i, t_i^f]$ ,  $i = 1, 2, 3, 4$ :

$$\begin{aligned} \dot{x}_i &= v_i \cos(\theta_i) \\ \dot{y}_i &= v_i \sin(\theta_i) \\ \dot{\theta}_i &= \omega_i \\ \mathbf{x}_i(t_i^i) &= \mathbf{x}_i^0 \\ |\omega_i| &\leq \bar{\omega}_i \end{aligned} \quad (20)$$

where  $(x_i, y_i)$  is the position of vehicle  $i$ ,  $\theta_i$  is the heading of vehicle  $i$ , and  $v_i$  is the speed of vehicle  $i$ . The control input  $\mathbf{u}_i$  of vehicle  $i$  is the turning rate  $\omega_i$ , whose absolute value is constrained to be less than  $\bar{\omega}_i$ . For illustration purposes, we chose  $\bar{\omega}_i = 1 \forall i$ . We assume that  $v_i$  is constant for this example, but our method can easily handle the case where  $v_i$  is a control input. The Hamiltonian associated with each vehicle is

$$\begin{aligned} H_i(t, \nabla_{\mathbf{x}_i} V_i(\mathbf{x}_i, t), V_i(\mathbf{x}_i, t)) \\ = \min_i \{ v_i \nabla_x V_i(\mathbf{x}_i, t) \cos(x_i(t)) \\ + v_i \nabla_y V_i(\mathbf{x}_i, t) \sin(y_i(t)) + \nabla_{\theta} V_i(\mathbf{x}_i, t) \omega_i \} \end{aligned} \quad (21)$$

giving the optimal control

$$\omega_i(t) = -\bar{\omega}_i \frac{\nabla_{\theta} V_i(\mathbf{x}_i, t)}{|\nabla_{\theta} V_i(\mathbf{x}_i, t)|} \quad (22)$$

The vehicles have initial conditions and required time of arrivals as follows:

$$\begin{aligned} \mathbf{x}_1^0 &= (-0.5, 0, 0), & t_1^f &= 0 \\ \mathbf{x}_2^0 &= (0.5, 0, \pi), & t_2^f &= 0.2 \\ \mathbf{x}_3^0 &= \left(-0.6, 0.6, \frac{7\pi}{4}\right), & t_3^f &= 0.4 \\ \mathbf{x}_4^0 &= \left(0.6, 0.6, \frac{5\pi}{4}\right), & t_4^f &= 0.6 \end{aligned} \quad (23)$$

The initial configuration of this example is shown in Figure 5.

The target sets  $\mathcal{T}_i$  of the vehicles are all 4 circles of radius 0.1 in the domain. The centers of the target sets are at  $(0.7, 0.2)$ ,  $(-0.7, 0.2)$ ,  $(0.7, -0.7)$ ,  $(-0.7, -0.7)$  for vehicles  $i = 1, 2, 3, 4$ , respectively. The domain  $\Omega$  and obstacles  $\Omega_{obs}$  are the same as those of the example in Section V. The setup for this example is shown in Figure 8.

The joint state space of this system is twelve-dimensional, intractable for analysis using the HJI PDE (2). Therefore, we will repeatedly solve the HJI VI (8) to compute the reach-avoid sets from targets  $\mathcal{T}_i$  for vehicles  $i = 1, 2, 3, 4$ , in that order, with moving obstacles induced by vehicles  $j = 1, \dots, i-1$ . We will also obtain  $t_{i,i}$ ,  $i = 1, 2, 3, 4$ , the latest acceptable departure times for each vehicle in order to reach  $\mathcal{T}_i$  by  $t_i^f$ .

Figures 6, 7, and 8 show the results. The obstacles are shown in thick black lines and the target sets are shown in thick colored circles. The reach-avoid sets are shown in thin colored curves, the induced obstacles are shown as dashed circles, and the positions and headings of each vehicle are shown as colored arrows.

Since the state space of each vehicle is three-dimensional, the reach-avoid set would also be three-dimensional. To visualize the results, we take slices of the reach-avoid sets at the initial heading angle  $\theta_i^0$  of the vehicles. Figure 6 shows the reach-avoid set slices for the four vehicles at their respective latest acceptable departure times  $t_1^i = -1.12$ ,  $t_2^i = -0.94$ ,  $t_3^i = -1.48$ ,  $t_4^i = -1.44$  determined from our method. The obstacles in the domain  $\Omega_{obs}$  and the obstacles induced by other vehicles inhibit the evolution of the reach-avoid sets, carving out thin “channels” that separate the reach-avoid set into different “islands”. One can see how these channels and islands form by looking at the time evolution of the reach-avoid set, shown in Figure 7 for vehicle 3.

Finally, Figure 8 shows the resulting trajectories of the four vehicles. The subplot labeled  $t = -0.55$  shows all four vehicles in close proximity without collision: each vehicle is outside of the danger zone of all other vehicles. The actual arrival times of vehicles  $i = 1, 2, 3, 4$  are 0, 0.19, 0.34, 0.31, respectively. It is interesting to note that for some vehicles, the actual arrival times are earlier than the planned arrival times  $t_i^f$ ,  $i = 1, 2, 3, 4$ . This is because in order to arrive at the target by  $t_i^f$ , these vehicles must depart early enough to avoid major delays resulting from the induced obstacles of other vehicles; these delays would have lead to a late arrival

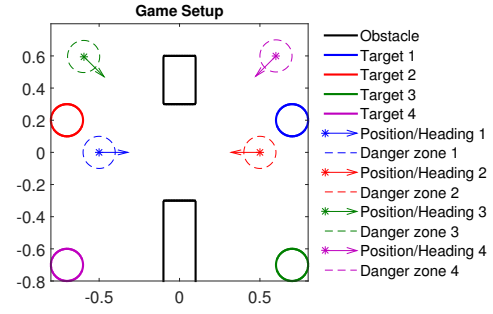


Fig. 5: Initial configuration of the four-vehicle example.

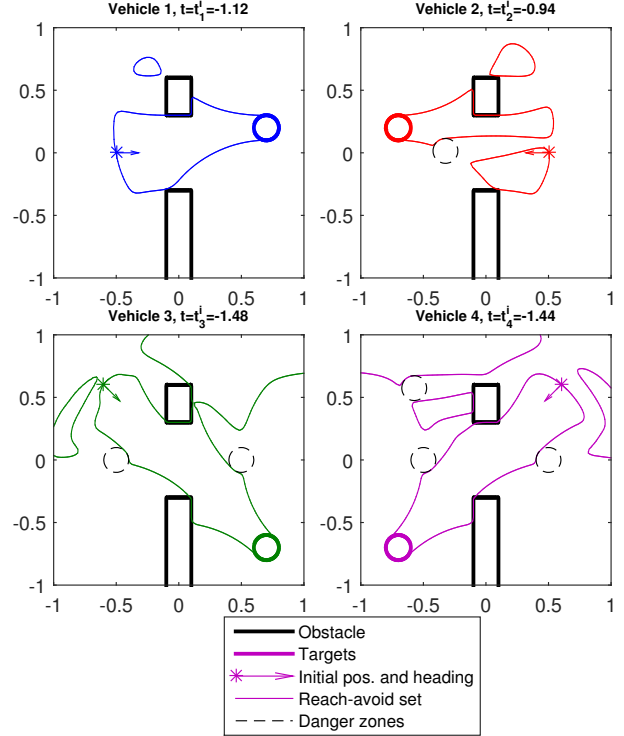


Fig. 6: Reach-avoid sets at  $t = t_i^i$  for vehicles  $i = 1, 2, 3, 4$ , sliced at the initial headings  $\theta_i^0$  of each vehicle. Since each vehicle has a maximum turn rate constraint, the presence of static obstacles  $\Omega_{obs}$  as well as time-varying obstacles induced by higher-priority vehicles  $\mathcal{O}_j^i(t)$  carves “channels” in the reach-avoid set, dividing it up into multiple “islands”.

if vehicle  $i$  departed after  $t_i^i$ .

## VII. CONCLUSIONS AND FUTURE WORK

We have presented problem formulation that allows us to consider the multi-vehicle trajectory planning problem in a tractable way by planning trajectories for vehicles in order of priority. In order to do this, we assumed lower-priority vehicles have knowledge of the trajectory of higher-priority vehicles, and modeled higher-priority vehicles as time-varying obstacles. We then solved a double-obstacle HJI VI that computes the reach-avoid set for each vehicle. The solution to the double-obstacle HJI VI characterizes the region from which each vehicle can arrive to its target

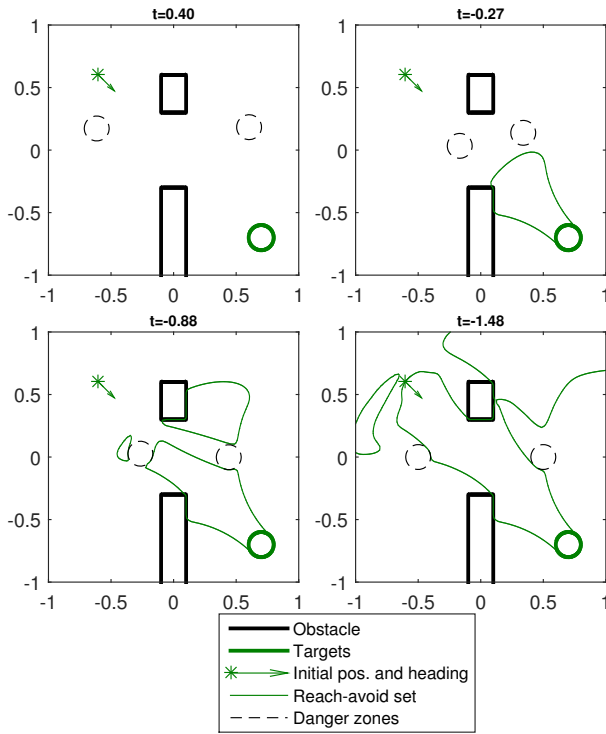


Fig. 7: Time evolution of the reach-avoid set for vehicle 3, sliced at its initial heading  $\theta_3^0 = \frac{7\pi}{4}$ . Initially, the reach-avoid set grows unobstructed by obstacles, as shown in the top subplots. Then, in the bottom subplots, the static obstacles  $\Omega_{obs}$  and the induced obstacles of vehicles 1 and 2,  $\mathcal{O}_1^3, \mathcal{O}_2^3$ , carves out “channels” in the reach-avoid set.

within a time horizon, while avoiding collision with higher-priority vehicles. The solution also gives each vehicle a latest acceptable departure time as well as the optimal control.

This paper provides a first application of the double-obstacle HJI VI. Immediate future work includes investigating ways to relax assumptions about the knowledge of the trajectories of other vehicles, more sophisticated induced obstacles for modeling trajectory uncertainty, problems involving adversarial agents, among other possibilities.

## REFERENCES

- [1] B. P. Tice, “Unmanned aerial vehicles – the force multiplier of the 1990s,” *Airpower Journal*, Spring 1991.
- [2] Amazon.com, Inc. (2014) Amazon prime air. [Online]. Available: <http://www.amazon.com/b?node=8037720011>
- [3] J. Stewart. (2014) Google tests drone deliveries in Project Wing trials. [Online]. Available: <http://www.bbc.com/news/technology-28964260>
- [4] Jointed Planning and Development Office (JPDO), “Unmanned aircraft systems (UAS) comprehensive plan – a report on the nation’s UAS path forward,” Federal Aviation Administration, Tech. Rep., September 2013.
- [5] W. M. Debusk, “Unmanned aerial vehicle systems for disaster relief: Tornado alley,” in *Infotech@Aerospace Conferences*, 2010.
- [6] P. Fiorini and Z. Shiller, “Motion planning in dynamic environments using velocity obstacles,” *International Journal of Robotics Research*, vol. 17, pp. 760–772, 1998.
- [7] G. C. Chasparis and J. Shamma, “Linear-programming-based multi-vehicle path planning with adversaries,” in *Proceedings of American Control Conference*, June 2005.

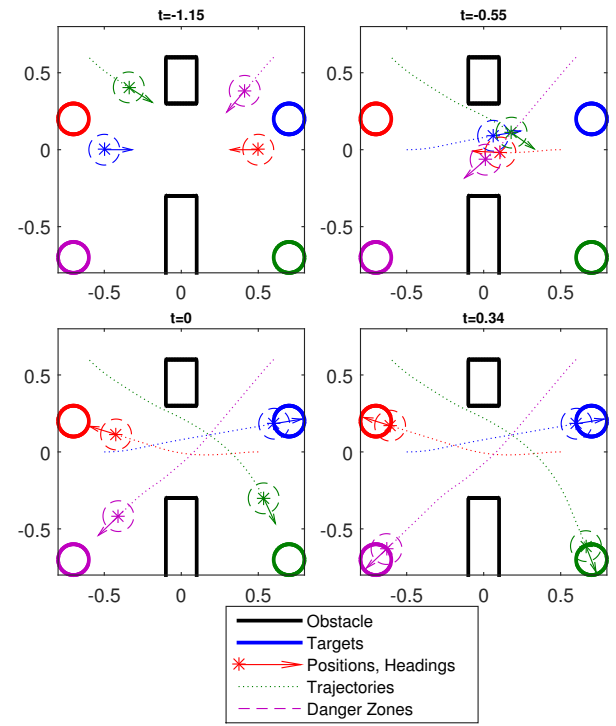


Fig. 8: The planned trajectories of the four vehicles. In the left top subplot, only vehicles 3 (green) and 4 (purple) have started moving, illustrating that  $t_i^f$  is not common across all vehicles. In the right top subplot, the four vehicles have come within very close proximity, but no vehicle is in the danger zone of other vehicles. In the left bottom subplot, vehicle 1 (blue) arrives at  $\mathcal{T}_1$  at  $t = 0$ , and in the right bottom subplot, all vehicles have reached their destination, some of them ahead of the scheduled time of arrival  $t_i^f$ .

- [8] R. Olfati-Saber and R. M. Murray, “Distributed cooperative control of multiple vehicle formations using structural potential functions,” in *IFAC World Congress*, 2002.
- [9] Y.-L. Chuang, Y. Huang, M. D’Orsogna, and A. Bertozzi, “Multi-vehicle flocking: Scalability of cooperative control algorithms using pairwise potentials,” in *Robotics and Automation, 2007 IEEE International Conference on*, April 2007, pp. 2292–2299.
- [10] I. Mitchell, A. Bayen, and C. Tomlin, “A time-dependent Hamilton-Jacobi formulation of reachable sets for continuous dynamic games,” *IEEE Transactions on Automatic Control*, vol. 50, no. 7, pp. 947–957, July 2005.
- [11] I. Mitchell, “Application of level set methods to control and reachability problems in continuous and hybrid systems,” Ph.D. dissertation, Stanford University, 2002.
- [12] E. Barron and H. Ishii, “The Bellman equation for minimizing the maximum cost,” *Nonlinear Analysis: Theory, Methods & Applications*, 1989.
- [13] O. Bokanowski, N. Forcadell, and H. Zidani, “Reachability and minimal times for state constrained nonlinear problems without any controllability assumption,” *SIAM Journal on Control and ...*, pp. 1–24, 2010.
- [14] J. A. Sethian, “A fast marching level set method for monotonically advancing fronts,” *Proceedings of the National Academy of Sciences*, vol. 93, no. 4, pp. 1591–1595, 1996.
- [15] S. Osher and R. Fedkiw, *Level Set Methods and Dynamic Implicit Surfaces*. Springer-Verlag, 2002, ISBN: 978-0-387-95482-0.
- [16] I. Mitchell, *A Toolbox of Level Set Methods*, 2009, <http://people.cs.ubc.ca/~mitchell/ToolboxLS/index.html>.
- [17] J. Ding, J. Sprinkle, S. S. Sastry, and C. J. Tomlin, “Reachability



- calculations for automated aerial refueling,” in *IEEE Conference on Decision and Control*, Cancun, Mexico, 2008.
- [18] H. Huang, J. Ding, W. Zhang, and C. Tomlin, “A differential game approach to planning in adversarial scenarios: A case study on capture-the-flag,” in *Robotics and Automation (ICRA), 2011 IEEE International Conference on*, 2011, pp. 1451–1456.
  - [19] O. Bokanowski and H. Zidani, “Minimal time problems with moving targets and obstacles,” *18th IFAC World Congress*, 2011.
  - [20] F. M. Callier and C. A. Desoer, *Linear System Theory*, 1998.
  - [21] M. Chen, Z. Zhou, and C. Tomlin, “Multiplayer reach-avoid games via low dimensional solutions and maximum matching,” in *Proceedings of the American Control Conference*, 2014.
  - [22] M. G. Crandall, L. C. Evans, and P. L. Lions, “Some properties of viscosity solutions of hamilton-jacobi equations,” *Transactions of the American Mathematical Society*, vol. 282, no. 2, p. 487, Apr. 1984.
  - [23] S. Osher and C.-W. Shu, “High-order essentially nonoscillatory schemes for hamilton-jacobi equations,” *SIAM Journal on Numerical Analysis*, vol. 28, no. 4, pp. pp. 907–922, 1991.
  - [24] S. Osher and R. Fedkiw, *Level Set Methods and Dynamic Implicit Surfaces*. Springer Verlag, 2003.
  - [25] C.-W. Shu and S. Osher, “Efficient implementation of essentially non-oscillatory shock-capturing schemes,” *Journal of Computational Physics*, vol. 77, no. 2, pp. 439 – 471, 1988.